Mekanika: Majalah Ilmiah Mekanika

Optimizing Energy Efficiency in Vertical Axis Wind Turbines: A CFD

Analysis of Inlet Velocity and Fluid Type Impact

Haris Nubli¹, Seung Jun Baek², Nabella Sofa Nur Afiqoh³, Yuki Trisnoaji³, Singgih Dwi Prasetyo^{3*}

- 1 School of Engineering, University of Surrey, Guildford, United Kingdom
- 2 Advanced-Green Technology Center, Korea Marine Equipment Research Institute, Busan, South Korea
- 3 Power Plant Engineering Technology, State University of Malang, Malang, Indonesia

Keywords: CFD ANSYS Fluent Vertical-axis wind turbine 2D design

Abstract

The development of Vertical Axis Wind Turbines (VAWTs) has become a key focus in renewable energy utilization due to their ability to operate at low wind speeds and their simple design. This study aims to analyze the effects of inlet velocity variations and fluid physical properties on flow patterns, turbulence, and kinetic energy in VAWTs. The simulation was conducted using the Computational Fluid Dynamics (CFD) method, based on ANSYS Fluent, for a 2D turbine model with a diameter of 12 cm. Inlet velocity variations of 10, 11, 12, 13, and 14 m/s were tested using three types of fluids: air, helium, and hydrogen. The results show that increasing inlet velocity transforms the flow pattern from stable to complex, with greater turbulence forming behind the cylinder. Air exhibited the highest kinetic energy at low to medium velocities, ranging from 10 to 12 m/s, which was up to 24.7% higher than that of helium and 3.8% higher than that of hydrogen. At higher velocities, 13–14 m/s, the kinetic energy difference among the three fluids decreased to less than 1.5%. Furthermore, outlet velocity was consistently higher than inlet velocity for all fluids, with hydrogen achieving the highest acceleration at 14 m/s.

1 Introduction

In the face of global challenges related to the energy crisis and climate change, the development of renewable energy technology is becoming increasingly urgent. One of the innovations that continues to be developed is the Vertical Axis Wind Turbine (VAWT) [1,2]. This technology attracts attention because it can work at low wind speeds and has a simpler design than horizontal turbines [3]. However, a thorough understanding of the impact of various technical factors, such as fluid type and inlet velocity, is necessary to achieve maximum efficiency. This article addresses these needs through a CFD-based simulation approach using ANSYS Fluent. Research on vertical-axis wind turbines has advanced significantly in tandem with progress in Computational Fluid Dynamics (CFD) simulations and the growing demand for sustainable energy solutions. ANSYS Fluent has become a widely used tool for simulating the performance of various VAWT designs [4]. For example, previous studies have demonstrated that blade design, fluid type, and inlet velocity parameters are critical factors affecting turbine efficiency [5,6].

https://dx.doi.org/10.20961/mekanika.v24i2.104188

Revised 17 July 2025; received in revised version 20 August 2025; Accepted 21 September 2025 Available Online 20 October 2025

2579-3144

© 2025 Mekanika: Majalah Ilmiah Mekanika. All right reserved

160

^{*}Corresponding Author's email address: singgih.prasetyo.fv@um.ac.id

Mesh resolution in CFD simulations plays a vital role in determining simulation accuracy [7-9]. Additionally, the selection of fluid type has a significant impact on turbine performance. At the same time, air is the most commonly used fluid, helium and hydrogen, with their lower density and higher thermal conductivity, present potential for enhanced efficiency [10,11]. Another study highlighted that varying inlet velocities can improve turbine power output up to a specific limit, beyond which excessive turbulence becomes problematic [12,13]. In terms of design, blade shapes like Darrieus and Savonius exhibit different efficiencies depending on wind speed and other operational conditions [14,15]. Blade design optimization can be further improved using a combination of CFD and genetic algorithms [16]. At the same time, twodimensional (2D) simulations are frequently used in preliminary studies due to their computational efficiency, even though three-dimensional (3D) simulations provide more realistic results [17,18]. The relationship between inlet velocity and the energy produced has also been a key focus in recent studies [19,20]. The relationship between inlet velocity and energy output is linear up to a certain speed, after which turbulence becomes dominant. Against this backdrop, this research focuses on the 2D simulation of verticalaxis wind turbines using three types of fluids: air, helium, and hydrogen [21,22]. Inlet velocity variations of 10, 11, 12, 13, and 14 m/s will be used to evaluate the relationship between inlet and outlet velocities and their influence on the kinetic energy produced [23,24]. The results of this simulation are expected to provide new insights into optimizing vertical-axis wind turbine designs to maximize energy efficiency, particularly for applications requiring specialized fluids [25,26].

With the increasing urgency for clean energy systems, various studies have been conducted to optimize the performance of wind turbines. Through the CFD simulation approach, researchers can examine how parameters such as inlet velocity, blade shape, and fluid type can affect the overall performance of the turbine [27,28]. In this context, selecting non-conventional fluids, such as helium and hydrogen, has become a new focus due to their unique physical properties. Previous studies have also demonstrated that mesh resolution and design optimization methods play a crucial role in enhancing the accuracy of simulation results. Research by Zhang and Janeway showed that mesh resolution is necessary in determining the accuracy of VAWT performance simulation [29]. Research by Siddiqui et al. studied the wake effects on wind turbines using a User Defined Function (UDF) [30]. It concluded that the type of fluid and system design parameters significantly influence the variation of flow characteristics. In terms of the influence of flow velocity parameters, it is reported that increasing the inlet velocity can significantly increase the turbine output power, but is followed by the emergence of excessive turbulence, which causes a decrease in efficiency at high speeds [30]. This is in line with the findings of research by Samaouali and Kadiri, which stated that the relationship between inlet velocity and output energy is linear up to a certain critical point, after which the effects of inertia and turbulence dominate [31]. Research by Fatahian et al. [32] applied a genetic algorithm to blade shape optimization and found that a blade design suited to specific wind conditions could improve turbine efficiency. On the same topic, research by Innocenti et al. [33] introduced the use of flexible blades was also investigated, and it was concluded that structural flexibility can contribute to the aerodynamic efficiency of the system. Additionally, alternative fluids such as helium and hydrogen are being explored, as noted in research by Mohamed et al. [34] which showed that lowdensity fluids can produce faster and more turbulent flow patterns, potentially improving or degrading system performance depending on operational conditions. Other research related to vertical wind turbines and ANSYS Fluent is summarized in Table 1.

While numerous studies have analyzed the aerodynamic performance of VAWTs, most have focused on conventional fluids such as air and a limited range of inlet velocities. Only a few works have systematically compared multiple low-density fluids, such as helium and hydrogen, across incremental inlet velocities to quantify their impact on flow patterns, turbulence characteristics, and kinetic energy output. This study bridges that gap by employing high-resolution 2D CFD simulations in ANSYS Fluent to directly correlate inlet velocity variations with both inlet—outlet velocity differentials and kinetic energy changes for three distinct fluids. The findings provide a unique dataset that enhances the understanding of fluid–structure interactions in VAWTs, offering practical insights for optimizing turbine performance in specialized operational environments.

Table 1. Previous research related to vertical wind turbines

| Deference | Table 1. Previous research related to vertical wind turbines | | | | | | | |
|-----------|--|---|--|--|--|--|--|--|
| Reference | Method | Key Result | | | | | | |
| [7] | CFD analysis of augmented VAWT (rotor + stator) using CFX 2020R2; National Advisory Committee for Aeronautics (NACA) 0018 aerofoil; varied mesh densities, time steps, and turbulence models; performance at $\lambda = 2.5$. | Augmented design improved output power 1.35× over open rotor; stator increased Cp and Ct by >36%; identified optimal mesh/time step with minimal computational cost; higher dynamic stall at low Tip Speed Ratio (TSR). | | | | | | |
| [35] | CFD simulation of NACA0018 VAWT blade using ANSYS Fluent; varied angle of attack (12°-15°) at constant wind velocity 8 m/s; SST k- ϵ turbulence model. | Optimum performance at 15° angle of attack with a lift coefficient of 1.689; uniform velocity distribution; validated via Cp–TSR curve; improved efficiency compared to a lower Angle of Attack (AoA). | | | | | | |
| [36] | 2D CFD simulation of H-Darrieus VAWT in ANSYS Fluent; tested various wind speeds; TSR variation to evaluate torque and power; NACA 0021 rotor profile. | Maximum torque 0.9365 Nm and power 19.6658 W at TSR = 0.9; torque coefficient ~10%, power coefficient ~9%; performance increases with TSR up to optimum, then declines. | | | | | | |
| [37] | Numerical modelling of VAWT with radial frames and flat blades using the k—ω turbulence model in ANSYS Fluent; 2D design with moving reference frame; targeted low wind speed operation. | Demonstrated suitability for low-wind- speed regions; model supports development of low-power, short-payback turbines for domestic/off-grid applications. | | | | | | |
| [38] | CFD modelling of VAWT using ANSYS Fluent; SolidWorks CAD for geometry; 2D simulation; analysis of aerodynamics and atmospheric wind flow physics. | Presented a theoretical and computational framework for VAWT design; validated the potential for low-wind applications; emphasized environmental benefits and feasibility in Uzbekistan. | | | | | | |

2 Method

Simultaneously, simulations were performed using ANSYS Fluent to obtain an accurate understanding of the fluid behavior in the turbine system. This method was chosen because it can visually represent fluid flow through a numerical approach. Variations in inlet velocity were applied, ranging from 10 to 14 m/s, with fluids including air, helium, and hydrogen. The turbine design was modeled in two dimensions to save computational time without reducing the validity of the results. All simulation steps were carried out systematically, from determining the initial parameters to analyzing the velocity and turbulence contours. In Figure 1, the flowchart illustrates the steps taken during the simulation using Ansys Fluent software. The simulation stage begins by opening ANSYS Fluent, the main application for modeling and numerical calculations. Furthermore, the main parameters that will be the focus of the research are identified. The fluids used for these parameters are air, helium, and hydrogen, each having a different density and viscosity. In addition, the turbine with a diameter of 12 cm is modeled to have a fluid inlet velocity of 10, 11, 12, 13, and 14 m/s. These parameters are chosen to represent typical wind speed conditions in the field and to assess how the system responds to changes in speed and fluid.

All the specified parameters are entered into the ANSYS Fluent interface, including geometry definition, turbulence model selection, boundary condition settings, and discretization method selection. After the configuration is complete, the simulation process is run. This process includes numerical iterations until the results reach scientifically acceptable convergence and stability.

Velocity contours, pressure, and flow pattern images are saved and analyzed after the simulation is complete. The analysis is conducted to compare the impact of each fluid and velocity variation on the distribution of kinetic energy and the output velocity. Quantitative data from the simulation results are arranged in tables and graphs to facilitate understanding [39,40]. The simulation procedure is summarized in Figure 1.

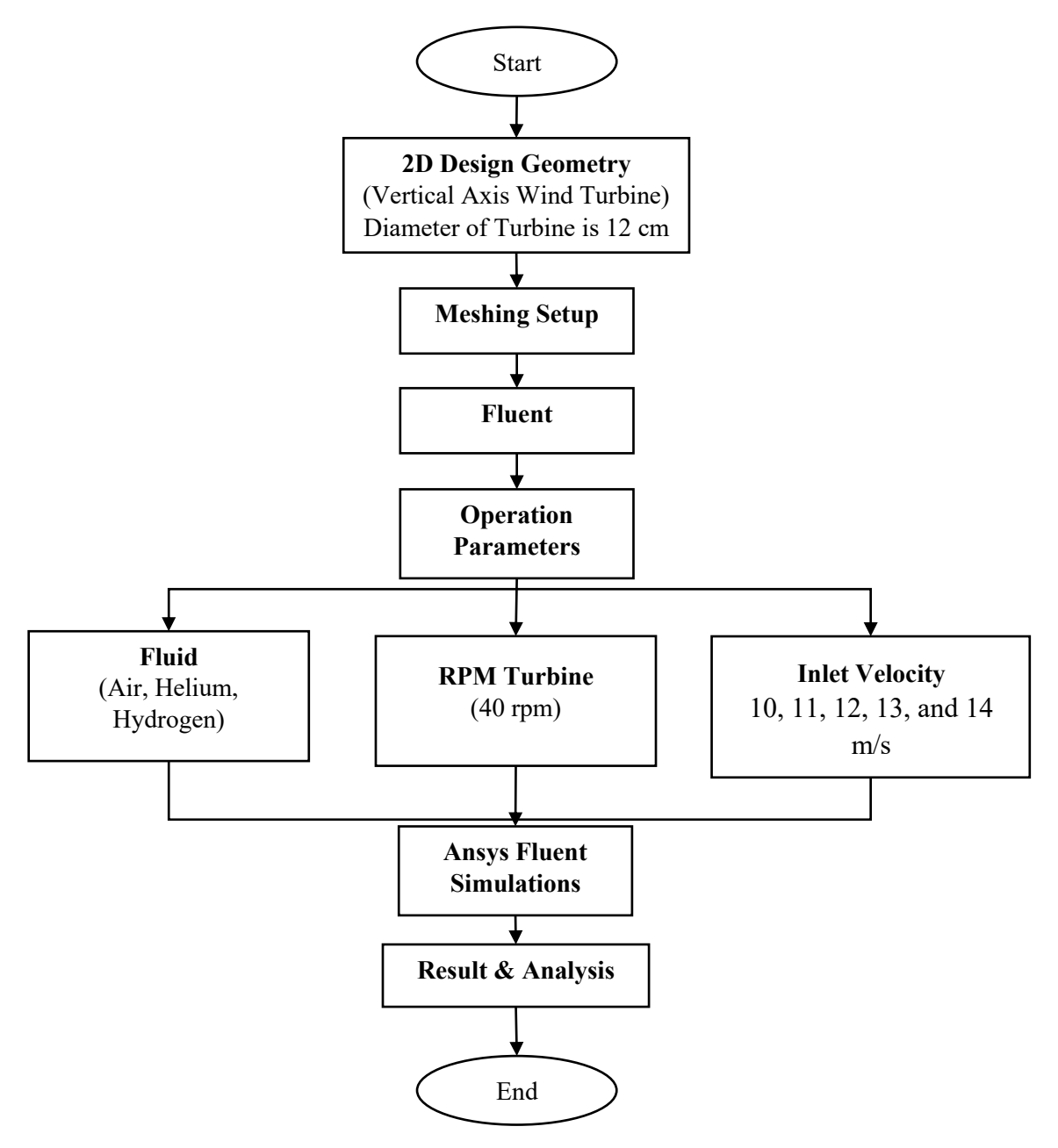


Figure 1. Flowchart of the proposed methodology

2.1 Boundary condition

Figure 2 illustrates the boundary conditions applied in the 2D simulation of a vertical-axis wind turbine. The incoming flow, with an initial velocity (v) of 10 m/s, is directed perpendicular to the turbine rotor, which has a diameter (D) of 12 cm and a blade chord length (c) of 2 cm. The rotor operates at an angular speed of 40 revolutions per minute (rpm). The types of fluid tested, along with their corresponding parameters, are detailed in Table 1. The variation in fluid physical properties influences velocity distribution, turbulence patterns, and the resulting kinetic energy, making these parameters critical for evaluating the effect of fluid characteristics on the turbine's aerodynamic performance.

Problem Specification

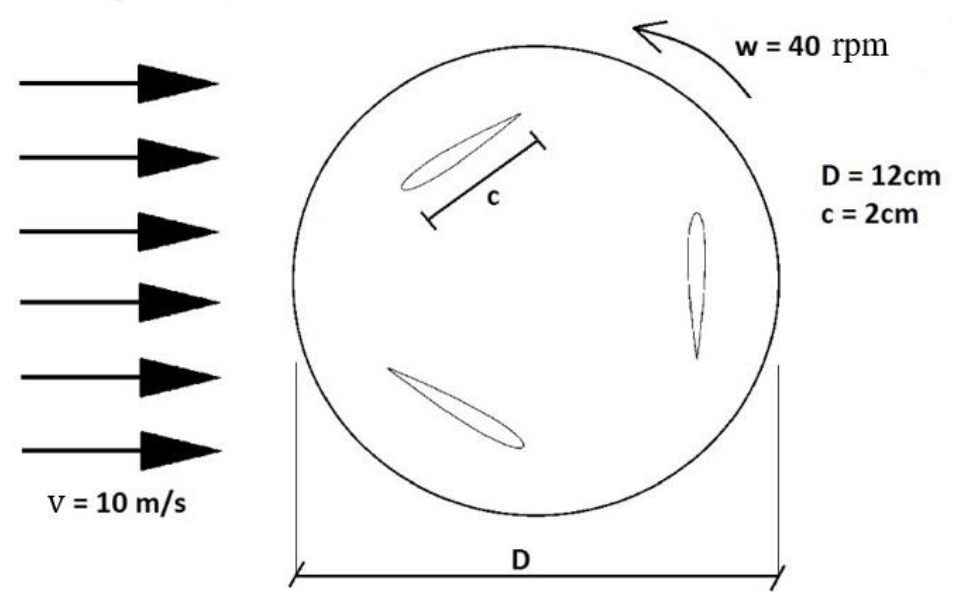


Figure 2. Boundaries of vertical wind turbine 2D

Table 1. Key parameters of the model

| Parameters of Fluids | Density (kg/m³) | | |
|----------------------|-----------------|--|--|
| air | 1.225 | | |
| helium | 0.1625 | | |
| hydrogen | 0.08189 | | |

2.2 Basic theory

The equations in this section are applied to calculate the kinetic energy of the fluid passing through the rotor's cross-sectional area under various inlet velocity and fluid type conditions. The calculation begins by determining the rotor's cross-sectional area from its diameter, as detailed in Equations 1 and 2, which is then used to compute the volumetric flow rate based on the inlet velocity, as shown in Equation 3. The mass flow rate is obtained by multiplying the fluid density by the volumetric flow rate, as shown in Equation 4. This mass value is combined with the square of the flow velocity to determine the kinetic energy using Equation 5. This procedure enables a quantitative assessment of how variations in fluid density and inlet velocity influence the kinetic energy produced. Therefore, these equations form the theoretical foundation that links the simulation input parameters to the resulting kinetic energy distribution, as detailed in the results and discussion section [41,42].

$$cross - sectional area = \pi r$$
 (1)

$$r = \frac{D}{2} \tag{2}$$

Where:

r: Fingers of cycle (m)

D: Diameter of cycle (m)

$$V = Cross - sectional area \times v$$
 (3)

$$m = \rho \times V \tag{4}$$

Where:

m: Mass (kg)

 ρ : Density (kg/m³)

 $V: Volume (m^3/s)$

$$K_E = \frac{1}{2}mv^2 \tag{5}$$

Where:

 k_E : Kinetic Energy

m: Mass(kg)

v: Velocity (m/s)

3 Results and Discussion

3.1 Contour

The simulation results show that the flow pattern and turbulence level are greatly influenced by the type of fluid and its inlet velocity. In the air, increasing velocity causes more intense turbulence at the back of the cylinder. Meanwhile, helium and hydrogen show higher velocity distributions at the same velocity, indicating the influence of lower density. The changes in the contour pattern of each fluid provide a clear picture of the flow dynamics around the turbine. Below are the simulation results, which display contour images of three different fluids: air, helium, and hydrogen, with inlet velocities of 10, 11, 12, 13, and 14 m/s, respectively. The contour images are displayed in Figure 3.

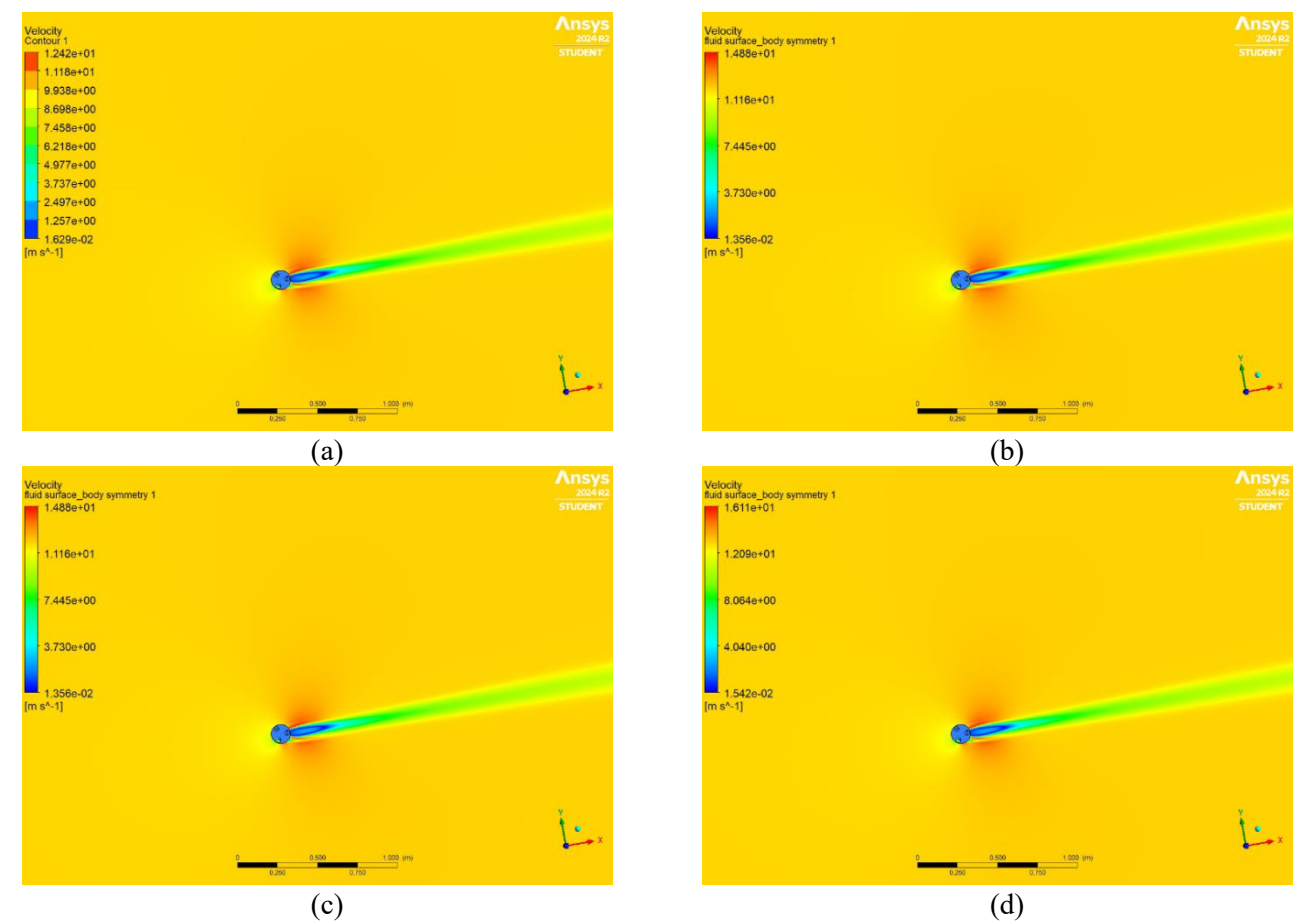


Figure 3. Contour of air: (a) Air 10 m/s, (b) Air 11 m/s, (c) Air 12 m/s, (d) Air 13 m/s, and (e) Air 14 m/s

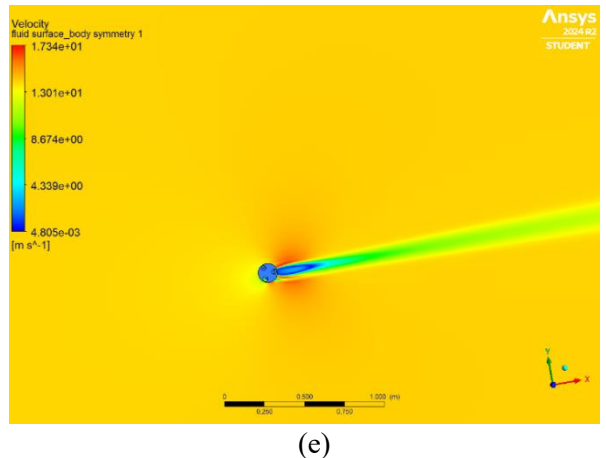


Figure 3. Cont.

Figure 3 presents the flow pattern around the cylinder, which is affected by the increase in airspeed. The air flows more slowly at an airspeed of 10 m/s, resulting in a low-velocity area in front of and behind the cylinder, characterized by a stable flow pattern and minimal turbulence. However, when the airspeed increases to 11 m/s, the air flows faster, causing a low-velocity area around the cylinder and turbulence at the rear. Around the cylinder, at a velocity of 12 m/s, there is a significant increase in velocity, accompanied by a larger area of turbulence behind it. At an airspeed of 13 m/s, there is faster flow and stronger turbulence behind the cylinder, and at an airspeed of 14 m/s, the air is distributed at a vast speed, with extreme turbulence behind the cylinder, which creates a more pronounced wake region behind the cylinder [43,44].

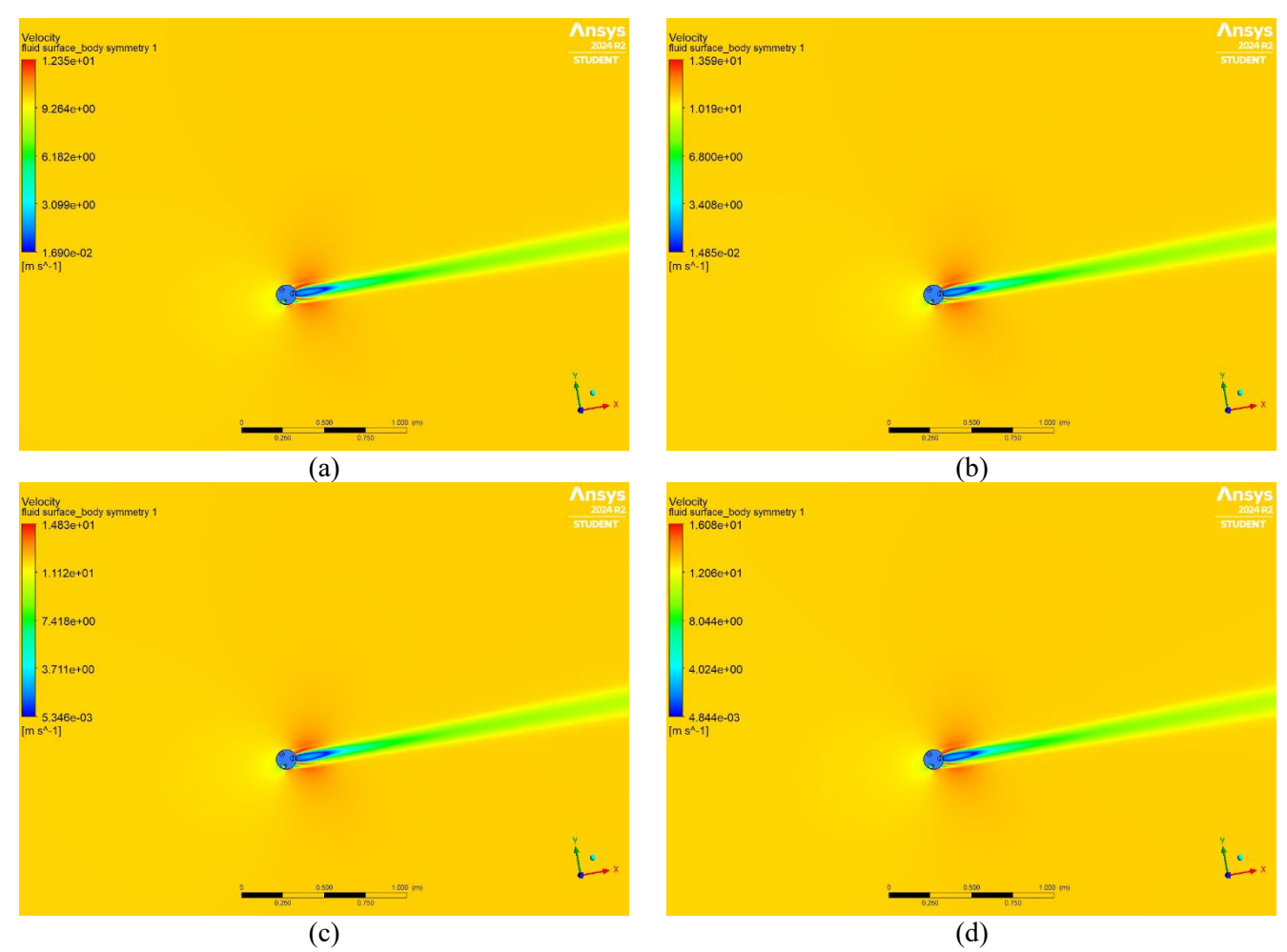


Figure 4. Contour of helium: (a) Helium 10 m/s, (b) Helium 11 m/s, (c) Helium 12 m/s, (d) Helium 13 m/s, and (e) Helium 14 m/s

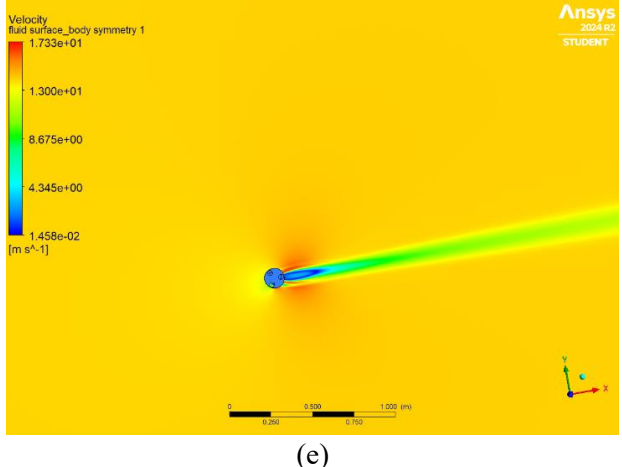


Figure 4. Cont.

Figure 4 illustrates the distribution of helium gas velocity around a circular source with varying inlet velocities. Helium flows slowly at 10 m/s, with the blue regions showing areas of low velocity and a more stable flow pattern. As the velocity increases to 11 m/s, the velocity distribution also increases, with the red areas indicating higher velocities and greater turbulence around the source. At 12 m/s, the velocity is much higher, with the dominant red regions showing very high velocity distributions and pronounced turbulence. At 13 m/s, the velocity distribution is even wider with larger turbulent areas around the source. Finally, at 14 m/s, the inlet speed is the highest, resulting in a broad velocity distribution and strong turbulence, indicating a highly disturbed flow. The analysis reveals that higher helium inlet speeds result in wider velocity distributions and increased turbulence around the source.

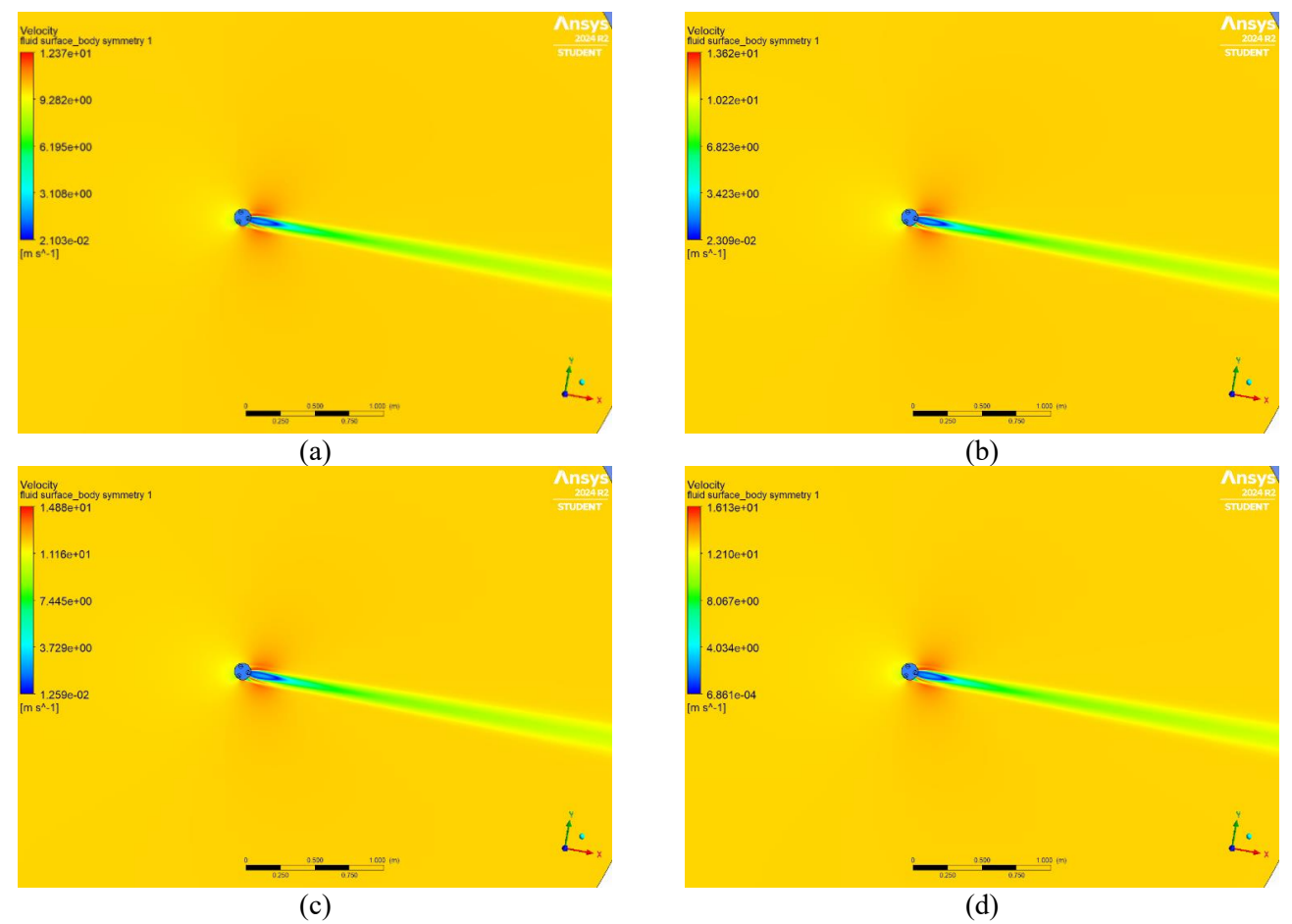


Figure 5. Contour of hydrogen: (a) Hydrogen 10 m/s, (b) Hydrogen 11 m/s, (c) Hydrogen 12 m/s, (d) Hydrogen 13 m/s, and (e) Hydrogen 14 m/s

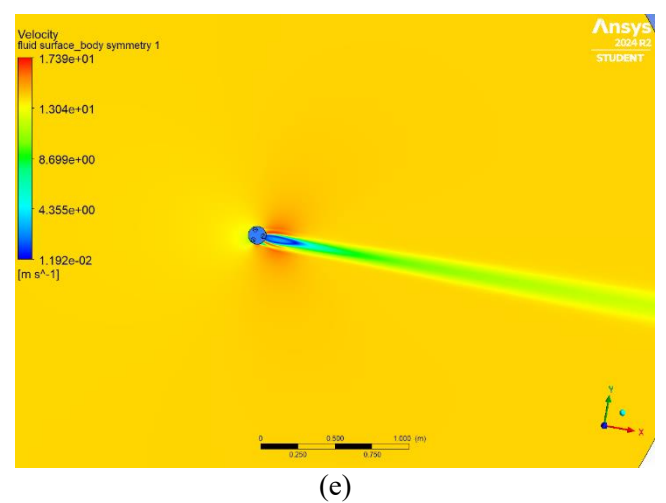


Figure 5. Cont.

3.2.2 Result summary

Table 2 presents the calculation of kinetic energy in this simulation, which is based on the fundamental laws of fluid physics. Combining data on density, cross-sectional area, and fluid velocity indicates the amount of energy the fluid possesses within the system. The formulas used are adjusted to two-dimensional conditions, assuming continuous flow, so that the simulation results remain relevant to real-world situations. For the three types of fluid used in this study air, helium, and hydrogen, the graph below illustrates the relationship between the inlet velocity (entry speed) in meters per second (m/s) and the kinetic energy in Joules. In general, kinetic energy increases with the inlet velocity of the fluid. The kinetic energy of air is greater than the kinetic energy of hydrogen and helium at a speed of 10 m/s. However, when the speed increases to 11 and 12 m/s, the kinetic energy of hydrogen approaches that of air, while the kinetic energy of air remains higher. The kinetic energy of helium always has the lowest kinetic energy value at all speeds. Figure 6 shows that the kinetic energy of the three fluids is almost the same at inlet velocities of 13 and 14 m/s, with the maximum values of air and hydrogen nearly the same, indicating that the difference in kinetic energy between fluids decreases at high speeds. According to this study, air, compared to hydrogen and helium, has greater kinetic energy at low to medium speeds. However, the kinetic energy of the three fluids tends to be almost the same at high speeds, probably due to the physical properties of each fluid, such as their density and ability to store kinetic energy.

Figure 7 shows the relationship between the inlet and outlet velocities of three types of fluids: air, helium, and hydrogen. The graph shows that the outlet velocities of each fluid tend to be greater than the inlet velocities, indicating an acceleration of the flow that changes in pressure or geometry of the system can cause. Hydrogen and air outlet velocities are the highest due to their lower densities, facilitating acceleration. Helium, which has a lower density than air, produces a higher outlet velocity than hydrogen but a lower one than air, indicating a linear relationship consistent with the principle of conservation of energy. The difference in outlet velocities between the fluids is greater at lower inlet velocities (10-11 m/s), but at higher inlet velocities (13-14 m/s), this difference is less significant due to the dominant inertial effect.

Table 2. Result of kinetic energy (Joules)

| Parameters of Fluid | 10 m/s | 11 m/s | 12 m/s | 13 m/s | 14 m/s |
|---------------------|--------|--------|--------|--------|--------|
| air | 13.2 | 22.85 | 22.85 | 29 | 36.1 |
| helium | 13.1 | 17.3 | 12.53 | 28.7 | 36 |
| hydrogen | 13.2 | 17.5 | 22.9 | 29.1 | 36.4 |

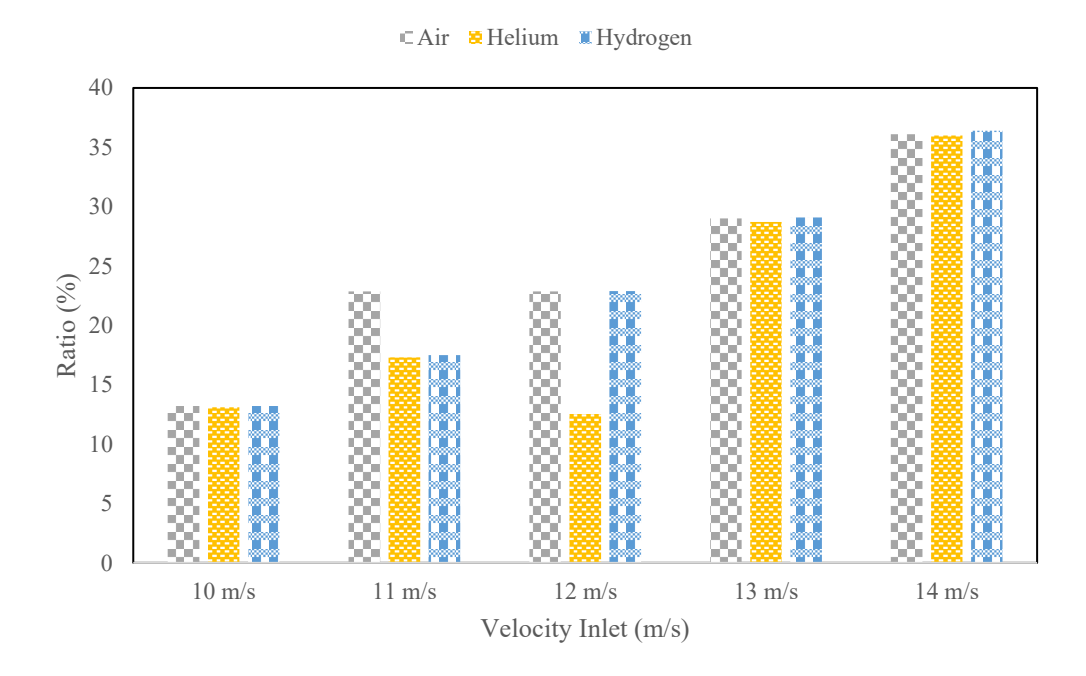


Figure 6. Graph of kinetic energy

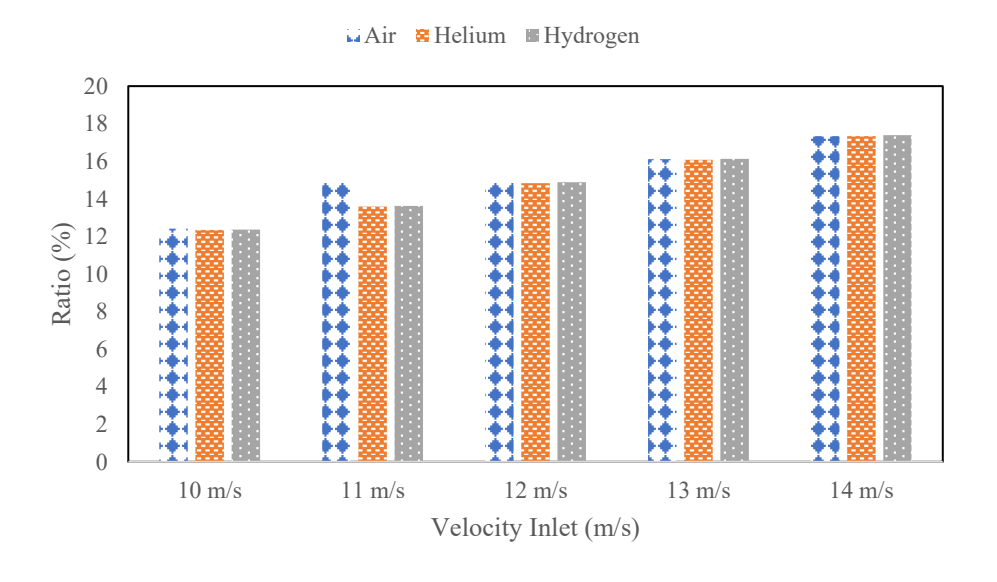


Figure 7. Graph of velocity outlet

4 Conclusions

This study successfully analyzed the effects of inlet velocity variations and fluid types on the aerodynamic performance of a vertical-axis wind turbine using CFD simulations in ANSYS Fluent. The inlet velocities tested ranged from 10 m/s to 14 m/s, while the fluids examined included air, helium, and hydrogen. The simulation results showed that increasing the inlet velocity significantly transformed the flow pattern from stable to complex, accompanied by higher turbulence levels in the wake region behind the rotor. Air tended to produce relatively controlled flow patterns at low velocities, but turbulence intensified sharply at higher speeds. Helium and hydrogen demonstrated a greater velocity distribution at the same inlet velocity compared to air, which is influenced by their lower densities. Differences in fluid physical properties were found to have a significant impact on flow response and the distribution of kinetic energy.

Kinetic energy calculations based on the simulation data revealed that at low to medium velocities (10-12 m/s), air exhibited the highest kinetic energy, up to 24.7% greater than that of helium and 3.8% greater than that of hydrogen. However, at higher velocities (13-14 m/s), the kinetic energy differences among the three fluids became negligible, with a difference of less than 1.5%. This phenomenon is attributed to the dominant inertial effects at higher speeds, which reduce the influence of density differences in the fluid. Furthermore, the outlet velocity of all fluids consistently exceeded the inlet velocity, indicating flow acceleration due to changes in pressure or rotor geometry. Hydrogen recorded the highest acceleration at 14 m/s, indicating its potential for applications requiring high flow acceleration. These findings highlight the importance of considering fluid physical properties in wind turbine design and optimization.

Overall, this research demonstrates that the combination of fluid type selection and inlet velocity adjustment can be leveraged to optimize the performance of vertical-axis wind turbines. The use of low-density fluids, such as helium and hydrogen, can provide advantages under specific operational conditions, particularly for enhancing flow acceleration. However, at low velocities, air remains superior in terms of kinetic energy. These results contribute to a deeper understanding of fluid–structure interactions in VAWT systems and can serve as a reference for the development of more efficient turbine designs. Future studies are recommended to explore the effects of blade geometry, variations in tip speed ratio, and three-dimensional simulations for more representative results. In addition, integrating this model with economic analysis could provide a more comprehensive view of its practical feasibility, enabling the development of wind turbine technology that is more adaptable to the needs of efficient and sustainable renewable energy.

5 Acknowledgement

This paper is the result of research entitled "Pengembangan Solar Tracker 2-Axis Dalam Peningkatan Konversi Energi Listrik Sel Surya Fotovoltaik," funded by the State University of Malang through the Penelitian Vokasional scheme with contract number 24.2.30/UN32.14.1/LT/2025.

References

- 1. S. Yagmur and F. Kose, "Numerical evolution of unsteady wake characteristics of H-type Darrieus Hydrokinetic Turbine for a hydro farm arrangement," *Appl. Ocean Res.*, vol. 110, article no. 102582, 2021.
- 2. M. S. Mauludin, M. Khairudin, R. Asnawi, Y. Trisnoaji, S. D. Prasetyo, S. R. Azizah, and R. T. Wiraguna, "In-depth evaluation and enhancement of a PV-wind combined system: A case study at the Engineering Faculty of Wahid Hasyim University," *Int. J. Power Electron. Drive Syst.*, vol. 16, no. 2, pp. 1274-1283, 2025.
- 3. W. A. Eltayeb and J. Somlal, "Performance enhancement of Darrieus wind turbines using Plain Flap and Gurney Flap configurations: A CFD analysis," *Results Eng.*, vol. 24, article no. 103400, 2024.
- 4. M. S. Mauludin, M. Khairudin, R. Asnawi, Y. Trisnoaji, S. D. Prasetyo, S. R. Azizah, and R. T. Wiraguna, "Assessing the Technological and Financial Feasibility of PV-Wind Hybrid Systems for EV Charging Stations on Indonesian Toll Roads," *Int. J. Sustain. Dev. Plan.*, vol. 20, no. 1, pp. 291-304, 2025.
- 5. L. Assaffat, M. S. Maulidin, Y. Trisnoaji, S. D. Prasetyo, M. A. Rizkita, Z. Arifin, and M. Choifin, "Improving Grid Stability with Hybrid Renewable Energy and Green Hydrogen Storage: A Study of Karimunjawa Island," *Math. Model. Eng. Probl.*, vol. 12, no. 5, pp. 1524-1534, 2025.
- 6. Y. Trisnoaji, S. D. Prasetyo, M. Choifin, C. Harsito, and A. Anggit, "Enhancing Efficiency in Small-Scale Hydropower: A Comprehensive Review of Archimedes Screw Turbine Design Innovations," *Semarak Eng. J.*, vol. 9, no. 1, pp. 1-15, 2025.
- 7. T. Wilberforce and A. Alaswad, "Performance analysis of a vertical axis wind turbine using computational fluid dynamics," *Energy*, vol. 263, article no. 125892, 2023.
- 8. T. Uchida, T. Yoshida, M. Inui, and Y. Taniyama, "Doppler Lidar investigations of wind turbine nearwakes and LES modeling with new porous disc approach," *Energies*, vol. 14, no. 8, article no. 2101, 2021.

- 9. Y. Trisnoaji, S. D. Prasetyo, M. S. Mauludin, C. Harsito, and A. Anggit, "Computational Fluid Dynamics Evaluation of Nitrogen and Hydrogen for Enhanced Air Conditioning Efficiency Computational Fluid Dynamics Evaluation of Nitrogen and Hydrogen for Enhanced Air Conditioning Efficiency," *J. Ind. Intel.*, vol. 2, no. 3, pp. 144-159, 2024.
- 10. Y. Zhang, X. Li, M. Barasa, and W. Xu, "CFD wind turbines wake effects by using UDF," *IOP Conf. Ser. Earth Environ. Sci.*, vol. 766, no. 1, article no. 012025, 2021.
- 11. H. A. Madsen, "An analytical linear two-dimensional actuator disc model and comparisons with computational fluid dynamics (CFD) simulations," *Wind Energy Sci.*, vol. 8, no. 12, pp. 1853-1872, 2023.
- 12. S. ed-D. Fertahi, T. Belhadad, A. Kanna, A. Samaouali, and I. Kadiri, "Assessment of fairing geometry effects on H-Darrieus hydro turbine performance using 2D URANS CFD simulations," *Energy Convers. Manag.*, vol. 293, article no. 117434, 2023.
- 13. S. J. Chemengich, S. Z. Kassab, and E. R. Lotfy, "Effect of the variations of the gap flow guides geometry on the savonius wind turbine performance: 2D and 3D studies," *J. Wind Eng. Ind. Aerodyn.*, vol. 222, article no. 104920, 2022.
- 14. S. L. Lee and S. J. Shin, "Structural design optimization of a wind turbine blade using the genetic algorithm," *Eng. Optim.*, vol. 54, no. 12, pp. 2053-2070, 2022.
- 15. S. Toudarbari, M. J. Maghrebi, and A. Hashemzadeh, "Evaluation of Darrieus wind turbine for different highway settings using CFD simulation," *Sustain. Energy Technol. Assessments*, vol. 45, article no. 101077, 2021.
- 16. S. D. Prasetyo, Z. Arifin, A. R. Prabowo, and E. P. Budiana, "The impact of cavity in finned thermal collector on PVT performance using Al2O3 nanofluid," *Int. J. Thermofluids*, vol. 27, no. June, article no. 101284, 2025.
- 17. A. Hijazi, A. ElCheikh, and M. Elkhoury, "Numerical investigation of the use of flexible blades for vertical axis wind turbines," *Energy Convers. Manag.*, vol. 299, article no. 117867, 2024.
- 18. H. A. Mrope, Y. A. C. Jande, and T. T. Kivevele, "A review on computational fluid dynamics applications in the design and optimization of crossflow hydro turbines," *J. Renew. Energy*, vol. 2021, no. 1, article no. 5570848, 2021.
- 19. V. Sebestyén, "Renewable and Sustainable Energy Reviews: Environmental impact networks of renewable energy power plants," *Renew. Sustain. Energy Rev.*, vol. 151, article no. 111626, 2021.
- 20. Y. Celik, D. Ingham, L. Ma, and M. Pourkashanian, "Novel hybrid blade design and its impact on the overall and self-starting performance of a three-dimensional H-type Darrieus wind turbine," *J. Fluids Struct.*, vol. 119, article no. 103876, 2023.
- 21. D. H. Didane, M. N. A. Bajuri, B. Manshoor, and M. I. Boukhari, "Performance Investigation of Vertical Axis Wind Turbine with Savonius Rotor using Computational Fluid Dynamics (CFD)," *CFD Lett.*, vol. 14, no. 8, pp. 116-124, 2022.
- 22. A. G. Auyanet, R. E. Santoso, H. Mohan, S. S. Rathore, D. Chakraborty, and P. G. Verdin, "CFD-based J-Shaped blade design improvement for vertical axis wind turbines," *Sustainability*, vol. 14, no. 22, article no. 15343, 2022.
- 23. S. ed-D. Fertahi, T. Belhadad, A. Kanna, A. Samaouali, I. Kadiri, and E. Benini, "A Critical Review of CFD Modeling Approaches for Darrieus Turbines: Assessing Discrepancies in Power Coefficient Estimation and Wake Vortex Development," *Fluids*, vol. 8, no. 9, article no. 242, 2023.
- 24. M. Akhlagi, F. Ghafoorian, M. Mehrpooya, and M. S. Rizi, "Effective parameters optimization of a small scale Gorlov wind turbine, using CFD method," *Iran. J. Chem. Chem. Eng. Res. Artic. Vol.*, vol. 42, no. 7, pp. 2286-2304, 2023.
- 25. J. Priyadumkol, B. Muangput, S. Namchanthra, T. Zin, T. Phengpom, W. Chookaew, C. Suvanjumrat, and M. Promtong, "CFD modelling of vertical-axis wind turbines using transient dynamic mesh towards lateral vortices capturing and Strouhal number," *Energy Convers. Manag. X*, vol. 26, no. April, article no. 101022, 2025.

- 26. M. G. Sanda, M. Emam, S. Ookawara, and H. Hassan, "Techno-enviro-economic evaluation of on-grid and off-grid hybrid photovoltaics and vertical axis wind turbines system with battery storage for street lighting application," *J. Clean. Prod.*, vol. 491, article no. 144866, 2025.
- 27. A. Abdallah, M. A. William, N. A. Moharram, and I. F. Zidane, "Boosting H-Darrieus vertical axis wind turbine performance: A CFD investigation of J-Blade aerodynamics," *Results Eng.*, vol. 27, article no. 106358, 2025.
- 28. M. S. Abul-Ela, M. E. F. El-Refaie, and A. I. Sayed, "Enhancing vertical-axis wind turbine self-starting with distinctive blade airfoil designs," *J. Eng. Appl. Sci.*, vol. 72, no. 1, pp. 1-30, 2025.
- 29. C. Zhang and M. Janeway, "Optimization of turbine blade aerodynamic designs using CFD and neural network models," *Int. J. Turbomach. Propuls. Power*, vol. 7, no. 3, article no. 20, 2022.
- 30. M. S. Siddiqui, M. H. Khalid, A. W. Badar, M. Saeed, and T. Asim, "Parametric analysis using cfd to study the impact of geometric and numerical modeling on the performance of a small scale horizontal axis wind turbine," *Energies*, vol. 15, no. 2, article no. 505, 2022.
- 31. A. Samaouali and I. Kadiri, "CFD comparison of 2D and 3D aerodynamics in H-Darrieus prototype wake," *e-Prime-Advances Electr. Eng. Electron. Energy*, vol. 4, article no. 100178, 2023.
- 32. E. Fatahian, R. Mishra, F. F. Jackson, and H. Fatahian, "Optimization and analysis of self-starting capabilities of vertical axis wind turbine pairs: A CFD-Taguchi approach," *Ocean Eng.*, vol. 302, article no. 117614, 2024.
- 33. G. Innocenti, M. Marconcini, V. Michelassi, A. Ciani, T. Jurek, A. S. D. Greco, and R. Pacciani, "On the assessment of CFD assumptions for the preliminary design of a two-stage high-pressure turbine: Impact of unsteady effects on thermal loads," *Int. J. Heat Mass Transf.*, vol. 236, article no. 126243, 2025.
- 34. O. S. Mohamed, A. M. R. Elbaz, and A. Bianchini, "A better insight on physics involved in the self-starting of a straight-blade Darrieus wind turbine by means of two-dimensional Computational Fluid Dynamics," *J. Wind Eng. Ind. Aerodyn.*, vol. 218, article no. 104793, 2021.
- 35. S. Shukla, C. J. Ramanan, B. Jyoti Bora, A. Deo, and N. Alom, "Numerical analysis of vertical axis wind turbine blades in ANSYS Fluent," *Mater. Today Proc.*, vol. 59, pp. 1781-1785, 2022.
- 36. H. F. M. Yusri, F. A. Ramsay, T. W. Xuan, N. Z. Yong, P. M. Khai, D. H. Didane, and B. Manshoor, "2D Numerical Simulation of H-type Darrieus Vertical-Axis Wind Turbine (VAWT)," *J. Des. Sustain. Environ.*, vol. 5, no. 1, pp. 11-16, 2023.
- 37. M. Hamdamov, B. Bozorov, H. Mamataliyeva, and D. Ergashov, "Numerical modeling of wind turbine with vertical axis using turbulence model k ω in ANSYS FLUENT," *E3S Web Conf.*, vol. 401, article no. 02024, 2023.
- 38. I. Khujaev, O. Toirov, J. Jumayev, and M. Hamdamov, "Modeling of vertical axis wind turbine using Ansys Fluent package program," *E3S Web Conf.*, vol. 401, article no. 04040, 2023.
- 39. F. Plua, V. Hidalgo, P. A. L. Jiménez, and M. P. Sánchez, "Analysis of applicability of cfd numerical studies applied to problem when pump working as turbine," *Water*, vol. 13, no. 15, article no. 2134, 2021.
- 40. M. Carraro, F. D. Vanna, F. Zweiri, E. Benini, A. Heidari, and H. Hadavinia, "CFD Modeling of Wind Turbine Blades with Eroded Leading Edge," *Fluids*, vol. 7, no. 9, article no. 302, 2022.
- 41. M. H. A. Madsen, F. Zahle, S. G. Horcas, T. K. Barlas, and N. N. Sørensen, "CFD-based curved tip shape design for wind turbine blades," *Wind Energy Sci.*, vol. 7, no. 4, pp. 1471-1501, 2022.
- 42. M. M. Saad, S. Mohd, M. F. Zulkafli, N. A. Samiran, and D. H. Didane, "CFD simulation study on the performance of a modified Ram Air Turbine (RAT) for power generation in aircrafts," *Fluids*, vol. 6, no. 11, article no. 391, 2021.
- 43. A. Sharma, M. J. Brazell, G. Vijayakumar, S. Ananthan, L. Cheung, N. deVelder, M. T. H. de Frahan, N. Matula, P. Mullowney, and J. Rood, "ExaWind: Open-source CFD for hybrid-RANS/LES geometry-resolved wind turbine simulations in atmospheric flows," *Wind Energy*, vol. 27, no. 3, pp. 225-257, 2024.
- 44. M. S. Karaalioglu and S. Bal, "Performance prediction of cavitating marine current turbine by BEMT based on CFD," *Ocean Eng.*, vol. 255, article no. 111221, 2022.